WIRELESS COMMUNICATIONS AND MOBILE COMPUTING
Wirel. Commun. Mob. Comput. 2016; **16**:1078–1094
Published online 27 April 2015 in Wiley Online Library (wileyonlinelibrary.com). DOI: 10.1002/wcm.2588

RESEARCH ARTICLE

Goodput and throughput comparison of single-hop and multi-hop routing for IEEE 802.11 DCF-based wireless networks under hidden terminal existence

Canan Aydogdu[1]* and Ezhan Karasan[2]

[1] Department of Electrical and Electronics Engineering, İzmir Institute of Technology, 35430 Izmir, Turkey
[2] Department of Electrical and Electronics Engineering, Bilkent University, 06800 Ankara, Turkey

ABSTRACT

We investigate how multi-hop routing affects the goodput and throughput performances of IEEE 802.11 distributed coordination function-based wireless networks compared with direct transmission (single hopping), when medium access control dynamics such as carrier sensing, collisions, retransmissions, and exponential backoff are taken into account under hidden terminal presence. We propose a semi-Markov chain-based goodput and throughput model for IEEE 802.11-based wireless networks, which works accurately with both multi-hopping and single hopping for different network topologies and over a large range of traffic loads. Results show that, under light traffic, there is little benefit of parallel transmissions and both single-hop and multi-hop routing achieve the same end-to-end goodput. Under moderate traffic, concurrent transmissions are favorable as multi-hopping improves the goodput up to 730% with respect to single hopping for dense networks. At heavy traffic, multi-hopping becomes unstable because of increased packet collisions and network congestion, and single-hopping achieves higher network layer goodput compared with multi-hop routing. As for the link layer throughput is concerned, multi-hopping increases throughput 75 times for large networks, whereas single hopping may become advantageous for small networks. The results point out that the end-to-end goodput can be improved by adaptively switching between single hopping and multi-hopping according to the traffic load and topology.

KEYWORDS
IEEE 802.11 DCF; analytical model; multi-hop; goodput; throughput; single-hop

***Correspondence**
Canan Aydogdu, Department of Electrical and Electronics Engineering, İzmir Institute of Technology, 35430 Izmir, Turkey.
E-mail: cananaydogdu@iyte.edu.tr

1. INTRODUCTION

The 'Internet of Things' vision and the tendency to put wireless networks in place of wired user-end networks are expected to transform current single-hop wireless networks into larger and denser multi-hop wireless networks in the next decade. However, large and dense wireless network structures are shown to have limited capacity [1–3] and, therefore, new techniques are necessary to enhance the network performance. Multi-hop routing, which allows coverage extension, may also be used as a means for improving goodput and throughput performance in such large and dense wireless networks when coupled with power control mechanisms.

The widespread Institute of Electrical and Electronics Engineers (IEEE) 802.11-based single-hop wireless networks at the user-end today are expected to transform into multi-hop networks in various applications in order to extend the range and handle the growing number of 'things', such as sensors, medical wireless equipments, and vehicles [4–6]. In September 2011, IEEE published the 802.11s amendment, which allows IEEE 802.11-capable devices to operate in a multi-hop mesh network. Despite the vast amount of studies on IEEE 802.11 performance analysis, previous works focus mainly on single-hop networks or on simplifying assumptions at the medium access control (MAC) layer for multi-hop networks such as optimal link scheduling, multiaccess scheme with no concurrent transmissions, or no hidden terminals. A thorough understanding of performance in such dense multi-hop networks requires a comprehensive IEEE 802.11 MAC layer analysis, which is developed in this article with a focus on comparison of performances of multi-hop or single-hop transmissions. In this article, we investigate the

basic question of how direct transmission (single-hopping) and multi-hop routing strategies affect the goodput and throughput in IEEE 802.11 distributed coordination function (DCF)-based wireless networks. We use the term average goodput to express the end-to-end successful packet delivery rate to the destination nodes at the network layer averaged over all nodes, whereas the term average throughput is used to express the hop-by-hop successful packet delivery rate at the link layer averaged over all links. We prefer to use the term 'goodput' instead of end-to-end throughput in order to avoid confusion with the hop-by-hop throughput.

In an IEEE 802.11-based wireless network where nodes have identical and omni-directional ranges, going from single-hopping to two-hop routing, increases the end-to-end delay, which decreases the goodput because only one of the two hops can be active at any time because of half-duplex operation. On the other hand, throughput is increased due to the decreased propagation delay over the shorter hop. From a network point of view, both the goodput and the throughput tend to increase due to spatial reuse of the spectrum when multi-hopping is employed and transmit power control is exercised. On the other hand, some factors impair the goodput performance with multi-hop routing, such as bit errors that accumulate at each hop, noise in the channel, increased sensitivity to fading over shorter links, longer hops used by multi-hop routing due to lack of optimally placed relay nodes, route overhead, and route maintenance [7]. Moreover, the goodput and throughput performances are affected by MAC-related issues such as carrier sensing, collisions, and retransmissions [8]. For example, the underlying mechanisms that increase collisions and retransmissions are different with single-hop and multi-hop routing: the main factor that increases collisions and retransmissions in a dense wireless network with single-hop routing is the increased number of contending stations and hidden terminals, whereas the increased traffic causes most of the collisions with multi-hop routing [9]. Hence, when the effects of collisions and retransmissions are considered, it is not straightforward to determine which routing strategy achieves the best goodput and throughput performances. The investigation of the effect of routing on goodput and throughput performances requires an analysis incorporating the MAC behavior.

Under a perfect scheduling and routing assumption, some earlier studies show that the network capacity increases with multi-hop routing [1,10,11], while some other studies contrarily show that direct transmissions result in larger network capacity [12,13]. The paradoxical effects of power control on the capacity of wireless networks are pointed out in [14], where a time division multiple access simulator, which considers exponential backoff and carrier sensing but not MAC mechanisms such as collisions, retransmissions, and packet drops, is used. The basic problem of whether to directly transmit or use multi-hop routes is investigated by analyzing the effects of power control and optimum hop distance on various metrics, such as the transport capacity [15], random access transport capacity [16], or aggregate multi-hop information efficiency [17], where distributed multiaccess contention schemes with no concurrent transmissions and no hidden terminals are assumed. Instead of the using these metrics, which correspond to the product of the aggregate throughput and the hop distance (and the spectral efficiency for aggregate multi-hop information efficiency), we use the aggregate throughput and goodput in this paper with the motivation that all traffic flows in the network have the same weight in total capacity of the network irrespective of the distance between source-destination nodes. Our study departs from these capacity related studies, where the optimal link scheduling and optimal routing assumptions or multiaccess contention schemes are replaced by a comprehensive modeling of the IEEE 802.11 DCF in multi-hop networks.

The primary contribution of this study is to show the effects of direct transmission and multi-hop routing strategies on the goodput and throughput performances of multi-hop wireless networks with an analysis incorporating an extensive MAC behavior of the IEEE 802.11 DCF under the presence of hidden terminals. The secondary contribution is the introduction of an analytical framework for calculation of the end-to-end goodput and link layer throughput in IEEE 802.11 DCF-based multi-hop wireless networks. Analytical goodput models proposed for single-hop IEEE 802.11 wireless networks [8,18–21] are not useful for analyzing goodput and throughput in large and dense multi-hop wireless networks, where spatial reuse is achieved with concurrent transmissions.

Goodput and/or throughput of IEEE 802.11 DCF-based *multi-hop* wireless networks are studied in [3,13,14,22–28]. Owing to the comparable complexity increase when switching from single-hop to multi-hop network architecture, these studies are based on either simulations [3,13] or simplified assumptions. For example, the hidden terminal effect is not considered in [15,22,23,28], whereas Barowski, Biaz, and Agrawal [23] additionally assumes that each node is either relay or source. The analysis in [26] accounts for intra-path interference (interference of simultaneous transmissions of different links of the same path) and does not take into account the inter-path interference (interference of simultaneous transmissions of different paths), and its applicability is limited to networks where other flows do not intersect with the intended path. Thus, this analysis considers only a small portion of hidden terminals that are on the intended path. The hidden terminal problem is included in the throughput analysis of IEEE 802.11 in [24] and [25], where only three-node and string topologies are considered, respectively. Moreover, these studies calculate the goodput or throughput under either saturated [15,23–26,28] or unsaturated traffic loads [22,27].

To the best of our knowledge, we present here the first analytical model for the calculation of goodput and throughput in multi-hop wireless networks that, works for arbitrary topologies, provides fairly accurate results for large range of traffic loads and studied network topologies,

considers hidden terminals, models both inter-path and intra-path interference, allows paths to cross each other, and allows each node to be both source and/or relay. A new concept is introduced in this article for calculation of goodput in multi-hop networks: the inter-successful-delivery-time of a node, which is basically the average time between two successive successful DATA packet deliveries from a source to all destinations. The analytical goodput model is based on the calculation of this concept, which provides a better understanding for the following goodput dynamics in multi-hop wireless networks: goodput is highly dependent on the interface queue dynamics. Under unsaturated traffic loads, goodput, which is inversely proportional to the inter-successful-delivery-time, depends on the arrival rate of packets and on the number of packets transmitted for a single successful delivery. On the other hand, MAC dynamics such as carrier sensing, collisions, retransmissions, exponential backoff, and hidden terminal effect govern the goodput under saturated traffic loads. The goodput and throughput model presented in this paper is developed on top of the analytical IEEE 802.11 DCF model introduced in [9], which provides the basic parameters of the distributed coordination function in multi-hop networks, such as the probability of collision, probability of transmission, and network allocation vector (NAV) setting probability.

The proposed analytical model, verified by simulations, is used to analyze the dependency of goodput and throughput on routing strategy and offered traffic. We assume that frame errors occur only because of collisions, while frame errors due to channel noise are neglected as in [29]. For large topologies considered, multi-hop transmissions are shown to achieve a higher throughput because of the increased number of parallel transmissions. In small irregular networks, the multi-hop route traverses a larger total distance than the direct transmission route compared with large irregular networks because of lower node density. Hence, routing over multiple short hops becomes ineffective because of the decreased likelihood of parallel transmissions under moderate traffic loads. As a result, single-hopping increases the throughput in small networks considered for moderate traffic loads, where retransmissions are not negligible. Goodput, on the other hand, is increased with direct transmissions in small networks for any traffic load. In large networks considered, multi-hop transmission increases the goodput under low-to-moderate traffic loads, whereas goodput drops significantly with multi-hop transmissions under heavy traffic loads because of excessive traffic congestion. Furthermore, the analytical goodput and throughput model proposed in this article for IEEE 802.11-based multi-hop networks provides significantly shorter run times compared with simulations, together with a flexibility in solving larger networks with no limitation on memory requirements introduced by simulations.

The assumptions of the proposed goodput and throughput models are discussed in Section 2. Analytical models for evaluating the goodput and throughput performances of IEEE 802.11 DCF-based networks are introduced in Section 3 and in Section 4, respectively. Numerical results obtained by using these analytical models and simulations are presented in Section 5.

2. PROBLEM MODEL AND ASSUMPTIONS

Some simplifying assumptions made by several previous studies [22–25,30–32] are also adapted here in order to provide an analytically tractable solution to the problem: (1) disk radio model, (2) Poisson offered traffic, (3) bit error-free channel, and (4) stationary nodes. No assumption is imposed either on the topology or on the traffic pattern. In order to compare the performances of routing strategies, a comparison is conducted using the same topology and traffic pattern where all nodes in the network are assumed to use the same routing strategy: each generated packet traverses a path of h hops. Nodes are assumed to conduct perfect power control with infinitely variable levels and transmit with the minimum required power to reach the next hop. Perfect power control assumption is used in order to limit interference and make a fair comparison between single-hop and multi-hop routing. The transmission range is assumed to be equal to the carrier sensing and interference ranges in order to obtain an analytically tractable model.

Each node is assumed to use the IEEE 802.11 DCF in conjunction with the request to send/clear to send (RTS/CTS) exchange as the MAC protocol, because the RTS/CTS handshake mechanism is shown to improve IEEE 802.11 performance in multi-hop wireless networks when hidden nodes are present despite the overhead and delay it introduces [33]. The IEEE 802.11-based multi-hop networks under investigation are composed of nodes, which are either located in a regular hexagonal topology or distributed uniformly in a random topology inside an area with a diameter that is at least four times the transmission range in order to let hidden terminals to exist. In case of a collision, packets are retransmitted according to binary exponential backof until the maximum retry count (M) is reached. At each transmission attempt of a node, regardless of the number of retransmissions, each packet collides with a conditional probability p, conditioned on the fact that the particular node is attempting a transmission. Packets are dropped after M unsuccessful retries, which occurs with probability p^M. Although the probability of collision, p, is different for each node and each link in an inhomogeneous wireless network, an average value of p is used in the DCF model in order to simplify the analysis [9]. The assumption of a constant p becomes more accurate as the number of nodes and contention window size increase, and the network topology becomes more homogeneous [30].

The existence of hidden terminals increases the probability of packet collisions in multi-hop wireless networks, which is handled in the calculation of p separately for each topology in the DCF model introduced in [9]. The exact

location of hidden terminals and the possibility that these hidden terminals send a packet which collides with the RTS and CTS frames are computed for each link and averaged over all links in each topology. Hidden terminals lie in the receiver exclusive region, where nodes hear the receiver but not the transmitter, and they cause collisions whenever: (a) an ongoing transmission of hidden terminals collides with the RTS frame resulting with a RTS collision and (b) hidden terminals start a transmission during the start of the CTS frame that may end up with a DATA collision. A semi-Markov chain model, which models the behaviour of each node in both transmission and reception modes, is used in order to compute the probability of collision introduced by the hidden terminals in [9].

In the analytical model, packets are also dropped because of overflow of the finite-sized interface queue (IFQ), which resides between MAC and physical layers, with probability $P_{ifq}(i)$ at each node i for $1 \leq i \leq N$, where N is the total number of nodes in the wireless network. In our model, a network-wide value is used for p in order to simplify the analysis, which corresponds to the average conditional collision probability taken over all links, whereas $P_{ifq}(i)$ is different for each node. We assume that the blocking probability at node $i, P_{ifq}(i)$, is independent and constant for all packets arriving at the interface queue.

Between each node pair (i,j) in the network, there is a Poisson traffic with rate $\lambda_o(i,j)$. The total traffic at node i is given by $\lambda_t(i) = \lambda_o(i) + \lambda_r(i)$, where $\lambda_o(i) = \sum_j \lambda_o(i,j)$ and $\lambda_r(i)$ is the total relay traffic. Hence, the arrival process into the IFQ of a node i is the superposition of the generated Poisson traffic, $\lambda_o(i)$ at node i and the total relay traffic, which arrives at node i. The total relay traffic is not Poisson because packets are dropped by either collision probability p or blocking probability P_{ifq}. In order to simplify the analysis, we assume that the relay traffic is Poisson so that the overall arrival process to an IFQ becomes Poisson with a rate denoted by $\lambda_t(i)$ for node i.

The IFQ is assumed to have a buffer size of K packets, including the packet in service, and packets in the IFQ are served using the first-in-first-out discipline with a single server. The MAC layer service time is a non-negative random variable denoted by random variable T_S, which has a discrete probability of $Pr(T_S = t_s(i))$ given by

$$\Pr\{T_S = t_s(i)\} = \begin{cases} (1-p)p^i & \text{if } 0 \leq i < m \\ p^M & \text{if } i = M \end{cases} \tag{1}$$

where

$$t_s(i) = \begin{cases} T_{ts} + iT_{tc} + \sum_{j=0}^{i+1} W_j \frac{\bar{\sigma}}{2} & \text{if } 0 \leq i < m \\ MT_{tc} + \sum_{j=0}^{M} W_j \frac{\bar{\sigma}}{2} & \text{if } i = M \end{cases} \tag{2}$$

W_j is the contention window size at backoff stage j, T_{ts} and T_{tc} are the durations of a single successful transmission and a single collision, respectively, given by

$$T_{ts} = T_{RTS} + T_{CTS} + T_{DATA} + T_{ACK} + 3SIFS + DIFS,$$
$$T_{tc} = T_{RTS} + CTStimeout + DIFS$$

where $T_{RTS}, T_{CTS}, T_{DATA}$, and T_{ACK} correspond to transmission times of RTS, CTS, DATA, and acknowledgement (ACK) packets, respectively. DIFS and SIFS are the DCF and short interframe spaces, and CTStimeout is the CTS timeout duration [34]. $\bar{\sigma}$ in (2) is the average NAV duration, different than the slot time, σ, defined in the specifications, given by

$$\bar{\sigma} = P_{succ}(T_{rs} + \sigma) + P_{coll}(T_{rc} + \sigma) + P_{idle}\sigma \tag{3}$$

where T_{rs} is the average NAV duration that contains at least one DATA reception and T_{rc} is the average NAV duration that does not contain any DATA reception. P_{idle} is the probability that NAV is not set, P_{succ} is the probability that NAV is set for a long duration given as T_{rs} and P_{coll} are the probabilities that NAV is set for a short duration given as T_{rc}, conditioned on the fact that the node does carrier sensing with zero NAV. In multi-hop IEEE 802.11 DCF-based networks, the discrimination between events that set the NAV for long and short durations is necessary instead of channel states, because the channel state perceived by a node may not be the actual state of the channel when hidden nodes exist [9]. For example, two concurrent successful transmissions in the channel of a node are perceived as a collision. Also, a node perceives a successful channel if it successfully receives an RTS or CTS frame that collides at the relevant receivers.

The IFQ is an M/G/1/K queue, which can be solved using the techniques in [35]. Let π_n represent the probability of n packets in the queueing system upon a departure at the steady state, and let $\mathbf{P} = [p_{ij}]$ represent the queue transition probability matrix:

$$\mathbf{P} = \begin{bmatrix} k_0 & k_1 & k_2 & \dots & k_{K-2} & 1 - \sum_{n=0}^{K-2} k_n \\ k_0 & k_1 & k_2 & \dots & k_{K-2} & 1 - \sum_{n=0}^{K-2} k_n \\ 0 & k_0 & k_1 & \dots & k_{K-3} & 1 - \sum_{n=0}^{K-3} k_n \\ \vdots & \vdots & \vdots & & \vdots & \vdots \\ 0 & 0 & 0 & \dots & k_0 & 1 - k_0 \end{bmatrix} \tag{4}$$

where k_n denotes the probability of leaving behind n packets upon a departure and is calculated as

$$\begin{aligned} k_n &= \Pr\{n \text{ arrivals during service time } T_S\} \\ &= \sum_{i=0}^{M} \frac{e^{-\lambda_t t_s(i)} (\lambda_t t_s(i))^n}{n!} \Pr\{T_S = t_s(i)\} \end{aligned} \tag{5}$$

π_n is obtained by the normalization equation and the balance equation $\pi P = \pi$. Let p_n represent the steady-state probability of n packets in the queueing system, which is obtained by [35]

$$p_n = \frac{\pi_n}{\pi_0 + \lambda_t E[T_S]},\ 0 \le n \le K-1$$
$$p_K = 1 - \frac{1}{\pi_0 + \lambda_t E[T_S]} \tag{6}$$

where $E[T_S]$ is the expected service time. The steady state probability of dropping packets at the interface queue, P_{ifq}, is equal to p_K:

$$P_{ifq} = p_K \tag{7}$$

This analysis is repeated for each node i in order to obtain $P_{ifq}(i)$. Also, the probability that the node's buffer is empty after the node finishes processing a packet in backoff, q, is given by

$$q = \pi_0. \tag{8}$$

The probability of collision p, the blocking probabilities $P_{ifq}(i)$ for $1 \le i \le N$, and the average NAV duration $\bar{\sigma}$ are the input parameters to the proposed goodput and throughput model described in the next section. These parameters are obtained through fixed-point iterations introduced in the DCF model in [9], which are summarized in the flowchart depicted in Figure 1.

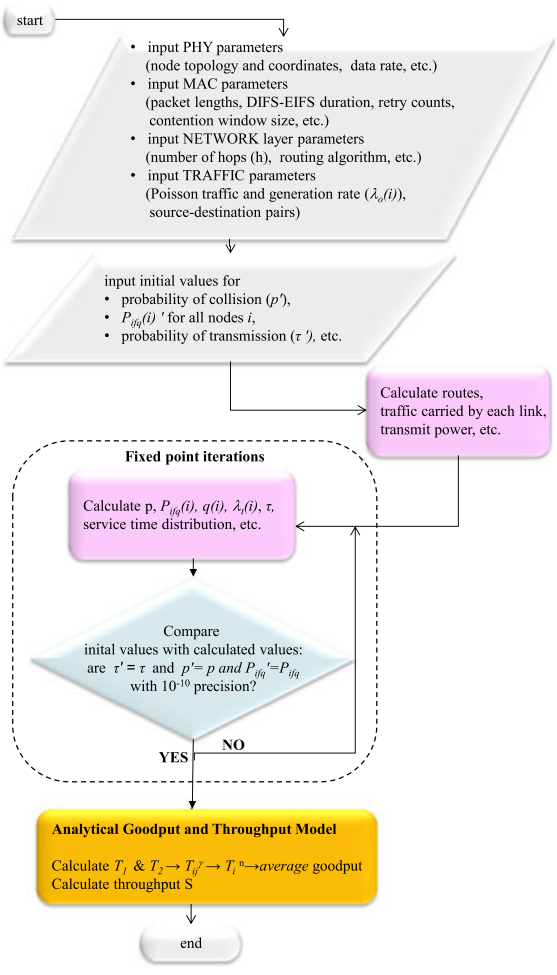

Figure 1. Flowchart for the proposed goodput and throughput models.PHY, physical layer; MAC, medium access control.

3. PROPOSED GOODPUT MODEL

In this section, we introduce an analytical goodput model for calculation of the average end-to-end goodput in arbitrary networks with arbitrary source destination pairs and traffic loads. The proposed goodput model consider a realistic MAC, where hidden terminals, carrier sensing, exponential backoff, freezing mechanisms, finite retry count, collisions, and retransmissions are included, and work for large traffic ranges and any two-dimensional topologies. Several challenges specific to multi-hop wireless networks that are considered in the proposed goodput model are as follows:

(1) Parallel transmissions over different paths may take place.
(2) Parallel transmissions over the same path may take place.
(3) Under light traffic loads, packet arrival rates shape the goodput, whereas under heavy traffic loads, MAC-specific parameters (such as backoffs, interframe space times, data rates, and packet durations) determine the goodput,
(4) Dropped packets due to finite IFQ buffer size and finite retry count affect the end-to-end goodput.

The proposed goodput model is based on calculating the duration between two successfully end-to-end deliveries of a source node, rather than calculating the number of successful deliveries per second, which is the conventional method used in the literature.

We first introduce the definitions and the basic equations of the proposed goodput model, and then the details of the model are presented.

3.1. Definitions

Let us denote the set of paths with source node i by Γ_i. Also denote the path from source node i to destination node j by γ_{ij}. In order to calculate the goodput, two definitions are made: the inter-successful delivery time over a path and the inter-successful delivery time of a node.

Definition 1. ***Inter-successful-delivery time over the path*** γ_{ij}, *denoted by* T_{ij}^{γ}, *is the average time between two successive successful DATA packet deliveries from the source node i to the destination node j.*

Definition 2. ***Inter-successful-delivery time for node*** i, *denoted by* T_i^n, *is the average time between two successive successful DATA packet deliveries from the source node i to any destination node of the paths in the set* Γ_i.

We then define the goodput of a node as follows.

Definition 3. ***Goodput of node*** *i, denoted by G_i, is the end-to-end successful delivery rate of DATA frames by source node i to the destination nodes of paths in the set Γ_i.*

Because G_i is the end-to-end successful delivery rate of DATA frames by source node i to any destination, it is proportional to the reciprocal of T_i^n, that is, the average time difference between end-to-end delivery of two successful DATA frames from source node i to any destination. Hence, goodput of node i is calculated by the following equation,

$$G_i = \frac{b_{DATA}}{T_i^n} \tag{9}$$

where b_{DATA} is the number of bits in a DATA frame.

Definition 4. ***Average goodput****, denoted by $\bar{G}$, is the average rate at which DATA frames are successfully delivered by source node i, averaged over all nodes i for $1 \leq i \leq N$.*

The average goodput is given by

$$\bar{G} = \frac{1}{N}\sum_{i=1}^{N} G_i \tag{10}$$

In order to obtain the average goodput, $\bar{G}$, or the goodput of any node, the inter-successful-delivery time of node i, T_i^n, for $1 \leq i \leq N$, needs to be computed, which will be discussed next.

3.2. Inter-successful-delivery time for a node

The calculation of T_i^n is illustrated by an example in Figure 2, where node i delivers packets to destination nodes a, b, and c, that is, $\Gamma_i = \{\gamma_{ia}, \gamma_{ib}, \gamma_{ic}\}$. The end-to-end successfully delivered packets are labeled by the corresponding destinations. The packets that are indicated by blank rectangles in the IFQ of node i are either

- packets with source node other than node i, which are forwarded by node i; and
- packets with source node i, which are dropped along the path (due to exceeding retry count or due to IFQ buffer overflow).

Let us decompose the packets in the IFQ of node i to sub-queues according to the destinations as shown in Figure 2. In this decomposition, the blank packets from source node i to node a, b, c are decomposed in the relevant sub-queues. The blank packets that do not originate from node i, but are forwarded by node i, are placed in one of the sub-queues, because this does not affect the results. $T_{ia}^{\gamma}, T_{ib}^{\gamma}$, and T_{ic}^{γ} are the inter-successful-delivery times over paths from source

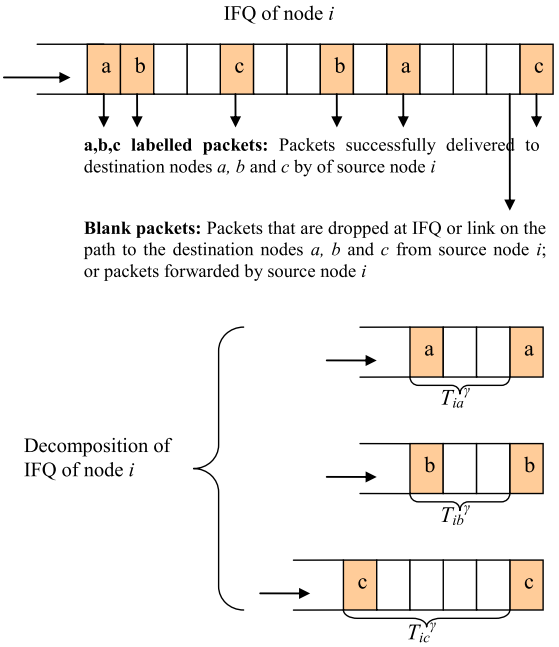

Figure 2. An example for illustration of calculation of T_i^n : T_i^n is calculated by averaging T_{ij}^{γ}, where $\Gamma_i = \{\gamma_{ia}, \gamma_{ib}, \gamma_{ic}\}$. IFQ, interface queue.

node i to destination nodes a, b, and c, respectively. Note that, T_i^n, which is the average time between two successfully end-to-end delivered DATA packets by source node i to any destination, becomes the reciprocal of the average of the reciprocal of inter-successful-delivery times over the paths in the set Γ_i, which is expressed by

$$T_i^n = \left(\sum_{j\in\Gamma_i} \frac{1}{T_{ij}^{\gamma}}\right)^{-1} \tag{11}$$

In order to calculate T_i^n, hence, the average goodput and the individual node goodputs, the inter-successful-delivery time of each path $\gamma_{ij} \in \Gamma_i, T_{ij}^{\gamma}$, is required, which will be calculated next. The rest of this section is devoted to calculation of T_{ij}^{γ}. The analytical IEEE 802.11 DCF model in [9] is used for calculation of the parameters $\bar{\sigma}, p$, and $P_{ifq}(i)$ for node i, which are used in the derivations in the succeeding sections.

3.3. Inter-successful-delivery time over a path

Inter-successful-delivery time over a path, T_{ij}^{γ}, is the average time between two successive successful DATA packet deliveries from the source node i to the destination node j. T_{ij}^{γ} is closely related to the offered load. Under unsaturated traffic loads, a second successful end-to-end delivery depends on the packet generation rate on the path γ_{ij}, $\lambda_o(i,j)$, whereas a second successful end-to-end delivery

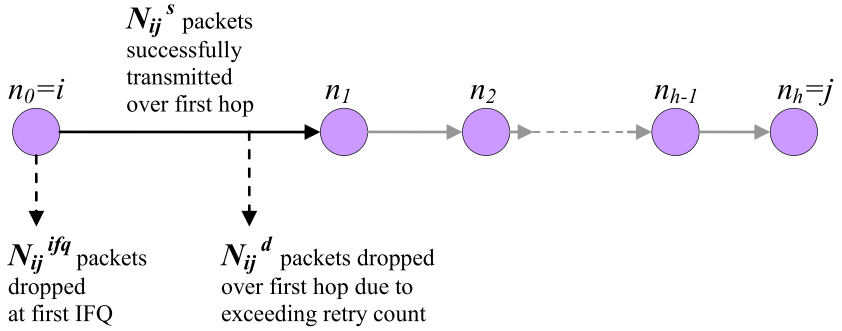

Figure 3. Illustration of number of successful/dropped packets over first hop of the h-hop path γ_{ij} : N_1^s, N_1^d and N_1^{ifq}. IFQ, interface queue.

depends on the time consumed by the dropped packets, including hop-by-hop successful packet transmissions that are dropped over some further link. The average time between two successive successful DATA packet deliveries from the source node i to the destination node j under unsaturated and saturated traffic loads are represented by T_{ij}^{unsat} and T_{ij}^{sat}, respectively. T_{ij}^{γ} is given by

$$T_{ij}^{\gamma} = max\left(T_{ij}^{unsat}, T_{ij}^{sat}\right) \tag{12}$$

The calculation of T_{ij}^{unsat} and T_{ij}^{sat} is given next.

3.3.1. T_{ij}^{unsat}.

Under unsaturated traffic loads, where there does not always exist a packet in the IFQ of node i for destination node j, the average time between two successive successful DATA packet deliveries from the source node i to the destination node j, becomes equal to T_{ij}^{unsat} and depends on the packet generation rate on the path $\gamma_{ij}, \lambda_o(i,j)$.

Over an h-hop path γ_{ij} with path nodes $n_0 = i, n_1, \ldots, n_h = j$, a packet is dropped at the kth IFQ with probability $P_{ifq}(n_{k-1})$ and at the kth hop with probability P_k^d; a packet is transmitted successfully over the kth hop with probability P_k^s, which is given by

$$P_k^d = p^M(1-p^M)^{k-1}\prod_{l=1}^{k}(1-P_{ifq}(n_{l-1})), 1 \le k \le h$$

$$P_k^s = (1-p^M)^k\prod_{l=1}^{k}(1-P_{ifq}(n_{l-1})), 1 \le k \le h \tag{13}$$

The probability of end-to-end successful packet delivery is equivalent to the probability of successful transmission over the last hop, P_h^s, which is as follows:

$$P_h^s = (1-p^M)^h\prod_{l=1}^{h}(1-P_{ifq}(n_{l-1})) \tag{14}$$

For a single end-to-end successful packet delivery, which occurs with probability P_h^s, the following number of packets are sent or dropped over the first hop of the path γ_{ij} on the average as illustrated in Figure 3:

- N_{ij}^{ifq} packets are dropped at the IFQ of the first node, that is, node i,
- N_{ij}^{s} packets are transmitted successfully over the first hop and
- N_{ij}^{d} packets are dropped due to maximum retry count.

For a single end-to-end successful packet delivery, which occurs with probability $P_h^s, 1/P_h^s$ packets are sent over the first hop of the path γ_{ij} or dropped at the first IFQ on the average. Among these $1/P_h^s$ packets, P_1^s/P_h^s of them are sent successfully over the first hop with probability P_1^s. N_{ij}^s is the average number of successful transmissions over the first hop of path γ_{ij} needed for one successful reception at the final destination j and is obtained by

$$N_{ij}^s = \frac{P_1^s}{P_h^s} = \frac{(1-p^M)^{1-h}}{\prod_{l=2}^{h}(1-P_{ifq}(n_{l-1}))} \tag{15}$$

Because N_{ij}^s successful transmissions over the first hop take place with probability $1-p^M$ for each packet, the average number of dropped packets over the first hop due to exceeding maximum retry limit becomes $\frac{p^M}{1-p^M}$ times the number of successful transmissions over the first hop, giving us

$$N_{ij}^d = N_{ij}^s\frac{p^M}{(1-p^M)} \tag{16}$$

Likewise, the average number of dropped packets at the first IFQ, N_{ij}^{ifq} is obtained as

$$N_{ij}^{ifq} = \frac{N_{ij}^s}{(1-p^M)(1-P_{ifq}(n_0))} \tag{17}$$

As a summary, one successful delivery from source node i to destination node j costs N_{ij}^s successful transmissions and N_{ij}^d dropped packets at the first hop and N_{ij}^{ifq} packet drops at the interface queue of node i. In other words,

a second successful end-to-end delivery is not possible before N_{ij}^{ifq} packets are dropped at the first IFQ, N_{ij}^{s} packets are transmitted successfully over the first hop, and N_{ij}^{d} packets are dropped over the first hop because of maximum retry count. Under unsaturated traffic, a second successful end-to-end delivery is not possible until $N_{ij}^{ifq} + N_{ij}^{s} + N_{ij}^{d}$ packets arrive IFQ of node i. T_{ij}^{unsat} is given by

$$T_{ij}^{unsat} = \frac{1}{\lambda_o(i,j)} \left(N_{ij}^{s} + N_{ij}^{d} + N_{ij}^{ifq} \right) \tag{18}$$

3.3.2. T_{ij}^{sat}.

As the traffic load increases, the average time between two successive successful DATA packet deliveries from the source node i to the destination node j, the duration for generating the necessary packets for one successful delivery becomes smaller than the time it takes until a second successful delivery over the path γ_{ij}. Calculation of T_{ij}^{sat}, the average inter-successful-reception time over the path γ_{ij} under saturated traffic loads, is illustrated in Figure 4, where packet transmissions of path nodes $n_0 = i, n_1, \ldots, n_h = j$ of an h-hop path γ_{ij} versus time are given.

T_{ij}^{sat} is composed of two terms:

$$T_{ij}^{sat} = T_1 + T_2 \tag{19}$$

where T_1 is the average time required to send all the packets over the first hop of the path γ_{ij} for a single end-to-end successful delivery and T_2 is the average time required for a single successful transmission to proceed over the next hops before another packet is sent by node i to the destination node j.

T_1 is calculated for saturated traffic loads, where IFQ of node i never becomes empty. Hence, it includes the average time required to complete N_{ij}^{s} successful transmissions and N_{ij}^{d} transmissions with failure. Because N_{ij}^{ifq} packet drops do not account for time consumption over the first hop of the path γ_{ij}, the time required to send $N_{ij}^{s} + N_{ij}^{d}$ packets over the first hop becomes

$$T_1 = N_{ij}^{s} T^{s} + N_{ij}^{d} T^{d} \tag{20}$$

where T^{s} is the average duration for one successful transmission and T^{d} is the average duration for one dropped packet over a link.

In this article, we propose a goodput model that consider a realistic MAC, where hidden terminals, carrier sensing, exponential backoff, freezing mechanisms, finite retry count, collisions, and retransmissions are included. Hence, T^{s} is the sum of the duration for one successful transmission plus the retransmissions that are less than

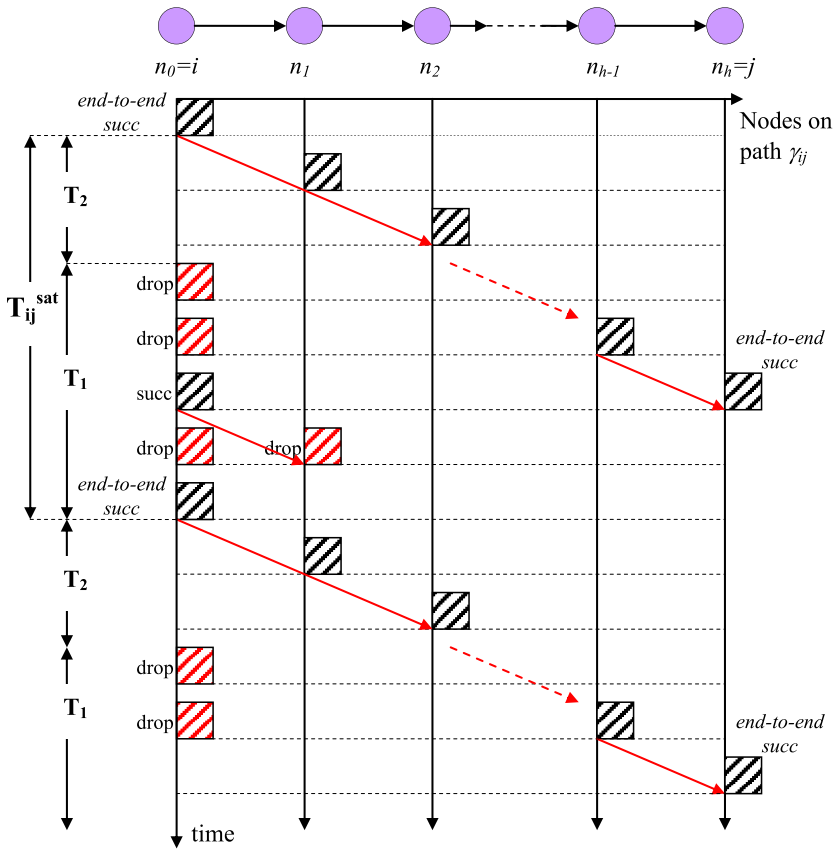

Figure 4. Illustration of calculation of T_{ij}^{sat}.

the maximum retry limit M, whereas T^d is equal to the duration of retransmissions exactly equal to M. T^s and T^d include the time spent for control packets, idle times due to backoff mechanisms and interframe spaces, given by:

$$\begin{aligned} T^s &= \bar{n}_M(DIFS + T_{RTS} + SIFS + T_{CTS} + EIFS) \\ &\quad + DIFS + T_{RTS} + T_{CTS} + T_{DATA} + T_{ACK} \\ &\quad + 3SIFS + T_{rb} + T_{sb} \\ T^d &= M(DIFS + T_{RTS} + SIFS + T_{CTS} + EIFS) \\ &\quad + T_{db} \end{aligned} \tag{21}$$

where EIFS is the extended interframe space and $\bar{n}_M$ is the average number of retries which is given by

$$\bar{n}_M = \sum_{i=0}^{M-1} ip^i(1-p) + Mp^M \tag{22}$$

T_{rb} is the average backoff duration during retries that results with a successful transmission, T_{sb} is the average duration of backoff after one successful transmission, and T_{db} is the average duration of backoff during one dropped packet because of exceeding retry count. T_{rb}, T_{sb}, and T_{db} are the corresponding backoff durations over a single link, which are given as

$$\begin{aligned} T_{rb} &= \sum_{b=0}^{\bar{n}_M} \frac{W_b}{2}\bar{\sigma} \\ T_{sb} &= \frac{W_0}{2}\bar{\sigma} \\ T_{db} &= \sum_{b=0}^{M-1} \frac{W_b}{2}\bar{\sigma} \end{aligned} \tag{23}$$

Note that the backoff counter is frozen for a duration of $\bar{\sigma}$, which is the average NAV duration. Hence, T_1 not only includes the duration of successful transmissions and failures over the first hop for one successful delivery but also it includes any received or overheard intra-path and inter-path packet transmissions in the neighborhood. Owing to the average NAV duration, which is computable by the DCF model introduced in [9], T_1 is the average time required to send all the necessary packets over the first hop of the path for a single successful end-to-end delivery, including the duration spent by node i during idle and receive modes.

In a multi-hop network under saturated traffic conditions, concurrent transmissions over a path may exist. Under the carrier sense multiple access/collision avoidance MAC scheme employed by IEEE 802.11, the transmissions over the second and third hops, if these hops exist, are dependent on the transmission over the first hop for a linear path with equal hop lengths, equal carrier sensing, and transmit ranges. An RTS transmission at the first hop is followed with a CTS transmission at the second hop, which blocks a concurrent RTS transmission at the third hop. Hence, successful parallel intra-path transmissions may occur beginning at the fourth hop along a path. For a wireless network with non-linear paths and non-equal hop lengths, which is the case studied in this article, the hop at which parallel inter-path transmissions may occur depends on the topology of the network. But in order to simplify the goodput analysis, we adapt an average analysis and assume that the independent intra-path transmissions start at the fourth hop along the path γ_{ij}. This assumption introduces an error on the goodput calculations, but this error is observed to be acceptable for different network topologies and different traffic scenarios illustrated by results presented in Section 5.

T_2 is the average time required for a single successful transmission to proceed over the next hops before another packet is sent by node i over path γ_{ij}. T_2 is not equal to the total end-to-end transmission delay for path γ_{ij}, rather it is the delay over the path γ_{ij} before an intra-path transmission takes place. As a result, T_2 becomes the average time required for one successful transmission to proceed over the second and third hops and waiting times at the interface queues of nodes n_1 and n_2 along the path γ_{ij}. Thus, T_2 is obtained as

$$T_2 = min(h-1,2)T^s + \sum_{k=1}^{min(h-1,2)} E[T_W](n_k) \tag{24}$$

where $E[T_W](n_k)$ is the expected waiting time at the IFQ of node n_k. The first term corresponds to time duration of a successful transmission over second and third hops, whereas the second term is the sum of average waiting times at IFQ of second and third nodes if they exist.

$E[T_W]$ of an M/G/1/K queue is calculated by summing up the waiting times for the packets in the queue and for the residual service time of the packet in service [35]:

$$E[T_W] = min(E[N_q] - 1, 0)E[T_S] + (1 - q_0)E[T_R] \tag{25}$$

where $E[N_q]$ is the expected number of packets in the system seen by an arrival that does join the IFQ, q_0 is the probability that an arrival that does join the system finds the queue empty, and $E[T_R]$ is the residual service time upon an arrival that does join the IFQ. In [35], the probability of n packets in system upon arrival that does join the system is denoted by q_n and the probability of n in system upon departure is denoted by π_n, and the following relation is given

$$\pi_n = q_n, 0 \leq n \leq K-1 \tag{26}$$

Thus q_0 becomes

$$q_0 = \pi_0 = q$$

which is also equal to q, that is, the probability of empty queue upon departure given by (8).

$E[N_q]$ is given by

$$\begin{aligned} E[N_q] &= \sum_{i=0}^{K-1} iq_i = \sum_{i=0}^{K-1} i\pi_i \\ &= \sum_{i=0}^{K-1} ip_i(\pi_0 + \lambda_t E[T_S]) \\ &= \left(\sum_{i=0}^{K} ip_i - KP_{ifq}\right)(\pi_0 + \lambda_t E[T_S]), \end{aligned} \tag{27}$$

where $\sum_{i=0}^{K} ip_i$ corresponds to average number of packets in the system denoted by $E[N_{sys}]$.

$E[T_R]$, the residual service time upon an arrival that joins the IFQ, is given by [35]

$$E[T_R] = \frac{E\left[T_S^2\right]}{2E[T_S]}. \tag{28}$$

Hence, (25) is expressed by

$$\begin{aligned} E[T_W] = (1-q)E\left[T_S^2\right]/(2E[T_S]) + min((E[N_{sys}] - KP_{ifq}) \\ \times (q + \lambda_t E[T_S]) - 1, 0)E[T_S]. \end{aligned} \tag{29}$$

Combining the results in (18)–(20) and (24), the inter-successful-delivery time over the h-hop path γ_{ij} is given by

$$\begin{aligned} T_{ij}^{\gamma} = max\Bigg(& \frac{1}{\lambda_o(i,j)}\left(N_{ij}^s + N_{ij}^d + N_{ij}^{ifq}\right), \\ & N_{ij}^s T^s + N_{ij}^d T^d + min(h-1,2)T^s \\ & + \sum_{k=1}^{min(h-1,2)} E[T_W](n_k)\Bigg). \end{aligned} \tag{30}$$

Having found the inter-successful-delivery time over path γ_{ij}, the goodput of node i and the average network goodput are obtained by using (11), (9), and (10).

4. THROUGHPUT MODEL

In this section, we present an analytical model for calculation of the link-layer throughput in multi-hop wireless networks. This model works for arbitrary topologies and large range of traffic loads while considering hidden terminals, with no assumptions on paths and node functionalities. We define the average node throughput as follows.

Definition 5. ***Average throughput*** *is the number of bits successfully transmitted per second by a node averaged over all links in the network.*

The average throughput includes all successfully delivered packets at the link layer; thus, any retransmission increases the average throughput. The calculation of average throughput is adapted from the IEEE 802.11 DCF-based analyses for single-hop networks [22,30] and for multi-hop networks [22], and the average throughput is given by:

$$S = \frac{\tau(1-p)b_{DATA}}{\bar{\sigma_n}} \tag{31}$$

where b_{DATA} is the number of bits of DATA packet including headers, τ is the probability of transmission, p is the collision probability, and $\bar{\sigma_n}$ is the average slot duration given by

$$\bar{\sigma_n} = \tau p T_{tc} + \tau(1-p)T_{ts} + p_{cs}\bar{\sigma}. \tag{32}$$

p_{cs} is the probability that a node executes carrier sensing when NAV is zero and is calculated by summing up the steady-state probabilities of all idle states of the discrete time Markov Chain model of IEEE 802.11 DCF introduced in [9].

5. GOODPUT AND THROUGHPUT COMPARISON OF SINGLE-HOP AND MULTI-HOP ROUTING

The goodput and throughput performances of routing strategies are studied for different topologies deployed in a fixed area: a hexagonally placed 127-node regular topology with $h = \{1,3\}$; a hexagonally placed 469-node regular topology with $h = \{1,2,3,6\}$; and 17 randomly generated topologies (10 with 10 nodes, 4 with 100 nodes, and 3 with 200 nodes) with $h = \{1,3\}$ are compared through analysis and simulations. For the hexagonal topologies, source-destination pairs are chosen such that all possible linear paths carry traffic, while for the random topologies, all source-destination pairs that have a three-hop path in between are chosen. The hexagonal topology is homogeneous in topology and traffic distribution, whereas the random topologies have no homogeneity. We use a simple channel model such that the received power decreases with d^{η}, where d is the distance from the transmitter and η is the path loss exponent. The simulations are conducted using Network Simulator 2, version ns-allinone-2.34 [36]. The parameters used for both the analytical model and the simulations are listed in Table I. Note that the data rate is fixed in this article, but it is a factor that impacts the transmission range and routing decision. The impact of various data rates on goodput and throughput performance is left as a future work.

The traffic load is classified as light, moderate, and heavy in this study based on the average number of times a frame is retransmitted, n_{rtx}, over a link as follows:

- Light traffic load: average number of retransmitted frames is negligible ($0 < n_{\text{rtx}} < 1$).
- Moderate traffic load: average number of retransmissions is not negligible but not high ($1 \leq n_{\text{rtx}} < M-1$), where M is the maximum retry count.

Table I. Parameters used for the analytical model and simulation runs.

Data rate	11 Mbps
Basic rate	1 Mbps
PLCP rate	1 Mbps
W_0	32
B	3
Short retry count	7
Long retry count	3
SlotTime	20 μs
DATA	1072 bytes
RTS	44 bytes
CTS	44 bytes
ACK	44 bytes
SIFS	10 μs
DIFS	50 μs
EIFS	412 μs
IFQ buffer size (K)	5 packets
RxSensitivity	−70 dBm
path loss exponent (η)	3

- High traffic load: average number of retransmissions is high ($M - 1 \leq n_{\text{rtx}}$).

5.1. Average goodput

The average goodputs of single-hop routing and multi-hop routing are computed by the analytical model and simulations for random topologies and are given for different network sizes in Figure 5, and for hexagonal topologies in Figure 6 as a function of the offered traffic. The analytical goodput model is applied to an error-free, non-fading channel where noise is neglected. Average goodputs in simulations are calculated by dividing the total number of bits of DATA frames successfully received at the network layers of all destinations by the simulation duration times the total number of nodes in the wireless network. The proposed goodput model provides fairly accurate results, which match with the simulations. The largest error is observed for a small interval of moderate traffic loads and for the 10-node highly irregular topology, where the error due to using an average value of p in the DCF model is largest. The error introduced by using an average p value for all nodes is more for random topologies compared with regular topologies.

The results show that under light traffic, single hopping and multi-hopping have very close goodputs, whereas goodput is maximized by direct transmissions for heavy traffic loads. For moderate traffic rates, the optimum routing strategy that maximizes the goodput depends on the network density. Among the networks considered in this study, for the 200-node random network, the 127-node and 469-node hexagonal networks, goodput increases with multi-hop routing for moderate traffic loads as seen in Figures 5(c), 6(a), and 6(b). For the 200-node random network, goodput increases up to 50%, for the 127-node hexagonal topology goodput is increased more than 160% and for the 469-node hexagonal topology goodput is increased up to 730% by multi-hopping compared with single hopping for moderate traffic rates. The average goodput obtained by using multi-hop routing substantially decreases as the offered load increases because of excessive congestion losses in the network. Because direct transmission is affected less with increasing offered load, single hopping yields significantly higher goodput than multi-hop routing at heavy traffic load. We also observe that, for all the topologies considered, goodput is maximized by either single-hop routing or multi-hop routing with the highest hop number. For the 469-node topology, it can be observed from Figure 6(b) that two-hop or three-hop transmissions never become advantageous when compared with single-hop and six-hop transmissions. Likewise, although not reported in this article, two-hop transmissions do not yield better results than direct and three-hop transmissions for the 127-node hexagonal and random topologies.

A comparison of the average goodputs of various network sizes in Figures 5 and 6 reveals that average goodput substantially decreases with growing network size for both single-hop and multi-hop routing. This suggests that for applications demanding high goodputs in very large dense ad hoc multi-hop networks, the IEEE 802.11b standard may not be a good choice, introducing a necessity for investigation of goodput for other IEEE 802.11-based standards, such as the IEEE 802.11ah [37].

5.2. Average throughput

The average throughput comparison of single-hop and multi-hop routing obtained from the analytical model and simulations are plotted for random topologies in Figure 7 and for hexagonal topologies in Figure 8. Average throughputs in simulations are calculated by dividing the total number of bits of DATA frames successfully received by the link layers of all nodes by the simulation duration times the number of nodes in the wireless network.

The accuracy of the analytical throughput model is observed to be quite well for large networks; however, inaccuracy increases for heavy traffic loads. The accuracy degrades also for the 10-node random network as observed in Figure 7(a), where single hopping may become more throughput efficient because of path inefficiency introduced by multi-hop routing. This is a parallel result with the capacity related study [12], where direct transmissions is shown to increase capacity for $N \leq 10$.

Average throughput is observed to increase with increasing traffic load until it becomes constant at heavy traffic loads, where packets are retransmitted/dropped because of increased congestion. The most important observation is that throughput is increased for multi-hopping for large networks ($N \geq 100$) as seen in Figures 7(b), 7(c), and 8. Throughput with multi-hopping is about more than twice of the throughput of single hopping under light traffic loads, and the gap further increases under moderate-to-

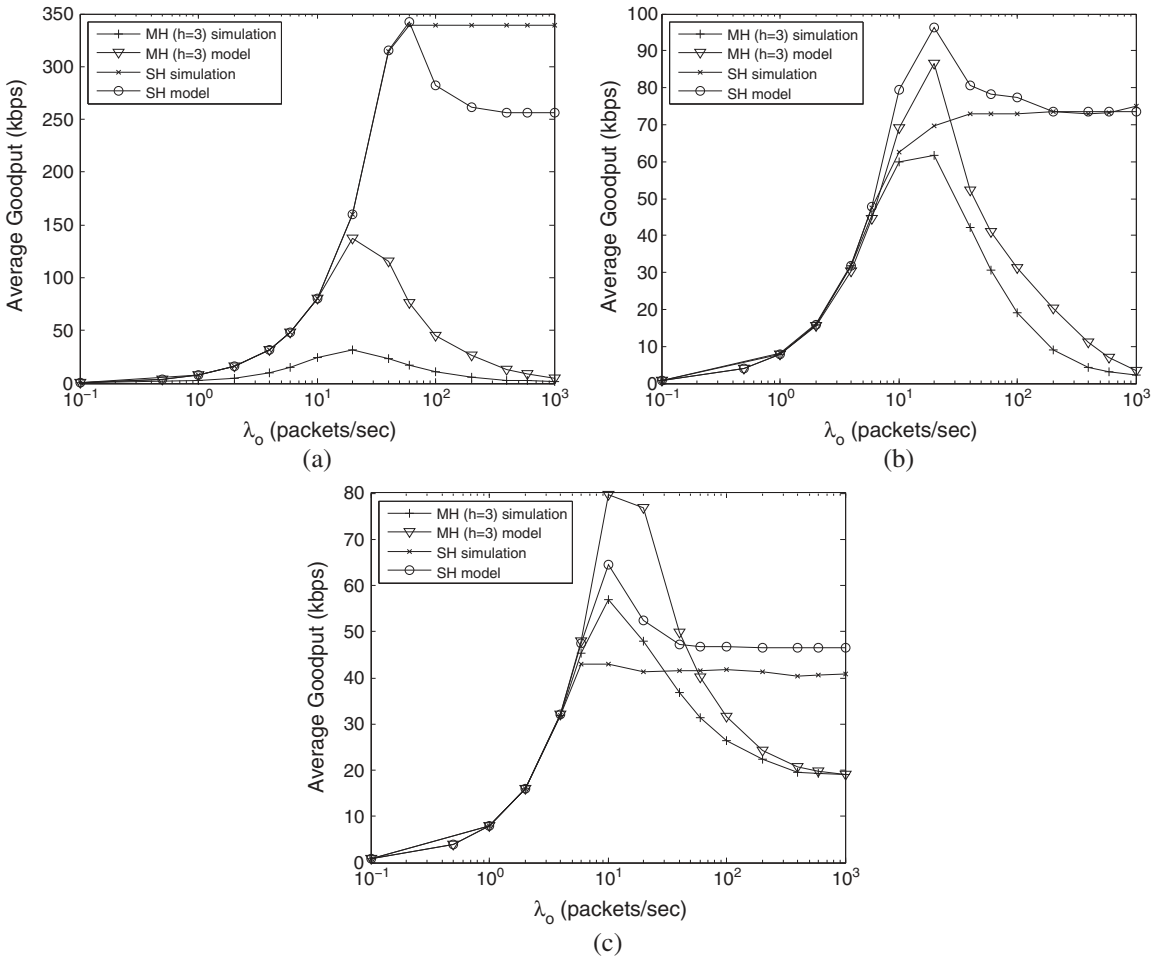

Figure 5. Average goodput comparison of single-hop (SH) and multi-hop (MH) routing obtained from the analytical model and simulations for (a) 10-node, (b) 100-node, and (c) 200-node random topologies.

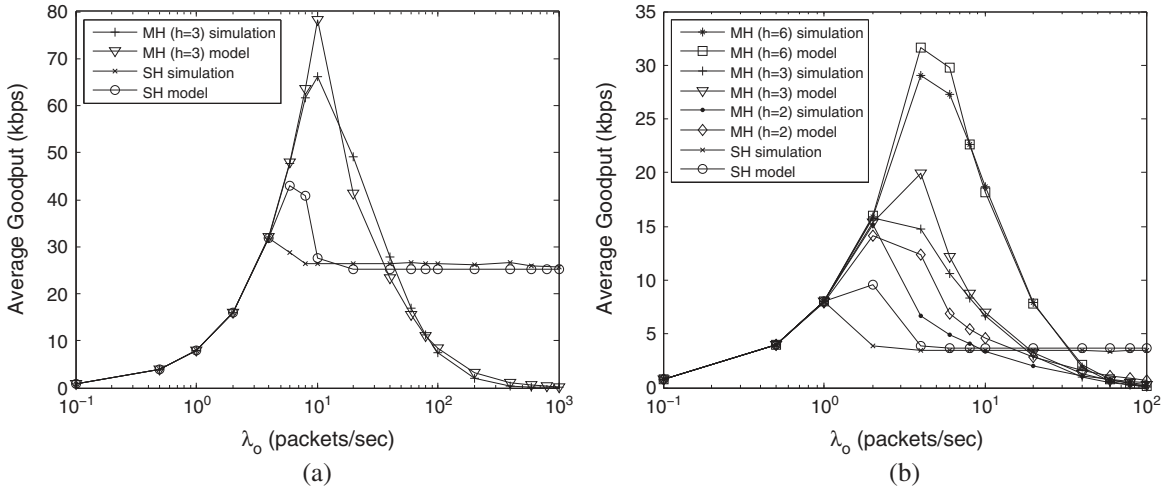

Figure 6. Average goodput comparison of single-hop (SH) and multi-hop (MH) routing obtained from the analytical model and simulations for (a) 127-node and (b) 469-node hexagonal topologies.

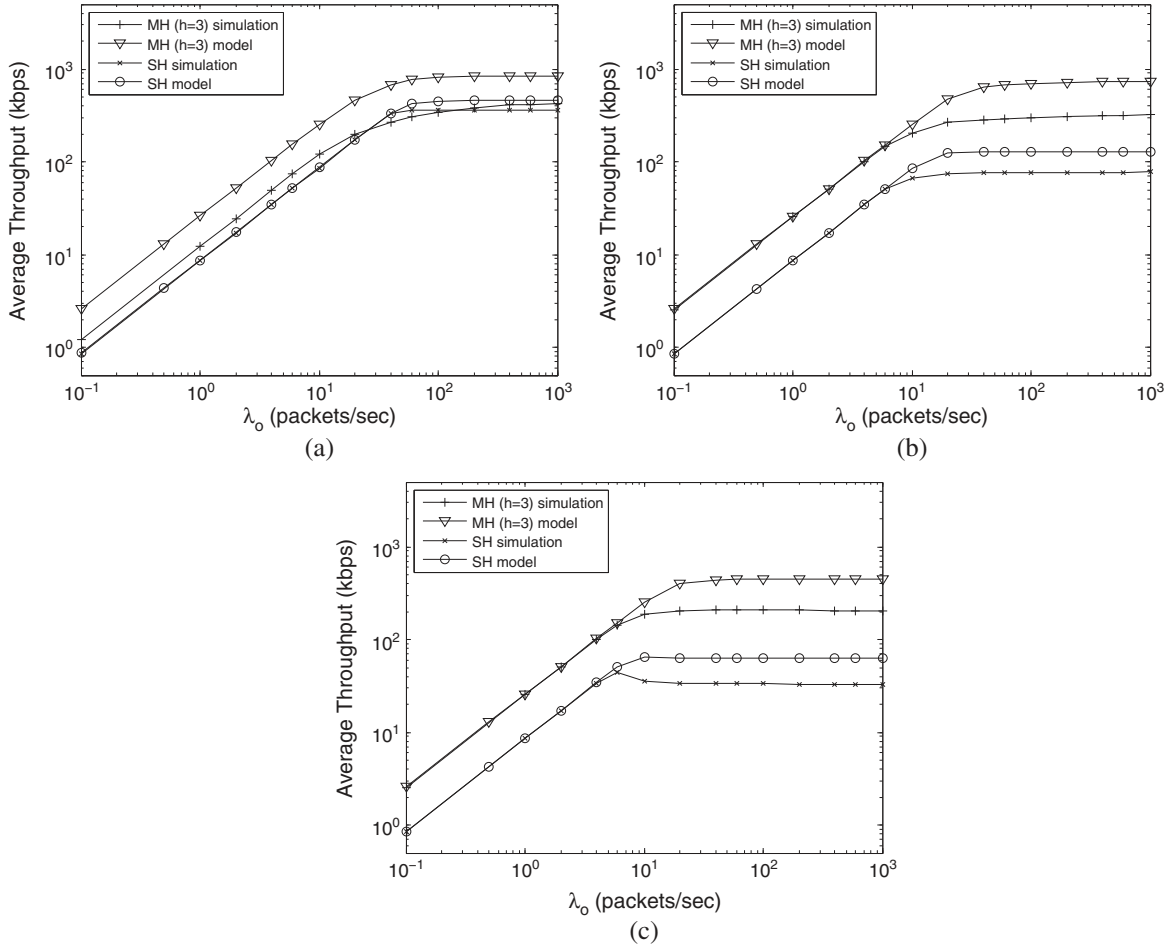

Figure 7. Average throughput comparison of single-hop (SH) and multi-hop (MH) routing obtained from the analytical model and simulations for (a) 10-node, (b) 100-node, and (c) 200-node random topologies.

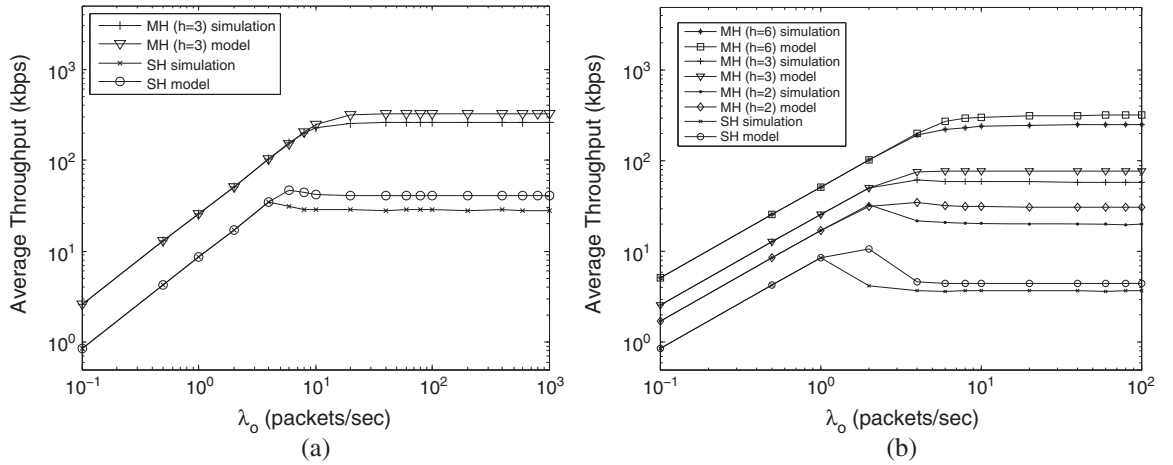

Figure 8. Average throughput comparison of single-hop (SH) and multi-hop (MH) routing obtained from the analytical model and simulations for (a) 127-node and (b) 469-node hexagonal topologies.

heavy traffic loads, where the effect of increased number of retransmissions is observed more. This gap is observed to increase more for larger networks and higher number of hops because of increased hop-by-hop transmissions.

Except the 10-node network under moderate traffic loads, throughput is maximized by multi-hopping with the highest hop count where the relative values of throughput of different routing strategies depend on the traffic load and hop count. Throughput of an h-hop route is observed to be h times that of direct transmission under light traffic loads, because each successful packet has to be sent h times in an h-hop route. However, throughput of an h-hop route becomes more than h times of the throughput with single-hopping because of packet retransmissions under moderate traffic loads. Under heavy traffic loads, the ratio of multi-hop to single-hop throughput becomes proportional to the maximum retry count, M.

The throughput and goodput of the direct transmission routing strategy have the same behavior because they differ only in terms of header bits, which are not counted in the calculation of goodput. Although throughput is an indicative of performance for only single-hop paths, goodput is an indicative of performance for both single-hop and multi-hop paths, which suggests that goodput should be considered as a performance metric in multi-hop wireless networks. Under moderate-to-heavy traffic loads, although more successful transmissions are observed along a path with multi-hop routing, the number of successful transmissions that reach the final destination is less compared with single-hop routing.

5.3. Run times for analytical model and simulations

The run time of the analytical calculations and simulations are compared in Table II for $\lambda_o = 1$ packets/sec for multi-hop routing for the hexagonal topologies and one instance of the random topologies. The simulation duration is taken to be equal to a duration required to generate an average of 6000 packets per node. The results are obtained on an Intel Xeon CPU X5355 at 2.66 GHz with a physical cache of 4096 KB and an RAM of size 16 GB with 8 GB swap. The numerical simulation results for goodput and throughput in this article are obtained by taking the average of 10 different 10-node-random topologies, four different 100-node-random topologies, and three different 200-node-random topologies, whereas the given run time for simulations belongs to a single instance of a random topology. Hence, the actual simulation run times are obtained by multiplying the given values by 10, 4, and 3 for the 10-node, 100-node, and 200-node-random topologies, respectively.

Table II. Comparison of run time of calculations of analytical IEEE 802.11 distributed coordination function model with simulations.

	Run time (sec)				
	Random topologies			Hexagonal topologies	
	N=10	N=100	N=200	N=127	N=469
Simulation	119,725	2999,148	5227,212	648,768	5670,547
Model	115,823	220,927	2361,916	167,370	147,961

The simulation run times for one instance are higher than the run time of DCF model calculations. The run time of the simulations and analytical DCF model increases in parallel with increasing size and irregularity of topologies. In terms of run time, the DCF model provides shorter run times compared with simulations. Furthermore, extensive simulations carried with different physical layer parameters and under higher number of nodes have shown that simulations obtained via Network Simulator 2 have memory problems, which limits the simulation duration, the number of nodes, the interface queue buffer size, and so on. Trial of different simulation durations have shown that limiting the simulation duration to smaller values results in incorrect results, due to the transient behavior of the network. Thus, all of the simulation results are obtained by removing the transient behavior of the network, which is done by removing the first half of the simulation duration and by taking the simulation duration equal to the duration required to generate an average of 6000 packets per node. The analytical DCF model proposed in this dissertation provides better run time and memory requirements, together with a flexibility in solving larger networks with no limitation on interface queue buffer size.

6. CONCLUSIONS

We have conducted a comparative analysis of the effects of single-hop and multi-hop routing on the goodput and throughput performances of IEEE 802.11 DCF-based multi-hop wireless networks under hidden terminal existence. Our analysis departs from similar studies by replacing some simplifying assumptions at the medium access control layer (optimal link scheduling, multiaccess scheme with no concurrent transmissions or no hidden terminals, etc.) by a comprehensive modeling of the IEEE 802.11 DCF in multi-hop networks, which takes carrier sensing, hidden terminals, intra-path and inter-path interferences, exponential backoff, finite retry limit, finite interface queue buffer sizes, packet drops, and so on into account. The analytical goodput and throughput models work for any two-dimensional topology with arbitrary source destination pairs and are shown to generate fairly accurate results under a large range of traffic loads.

The analytical results obtained via the proposed analytical models, supported by simulations, show that the effect of single-hop and multi-hop routing strategies on the goodput and throughput is network density and traffic load dependent. Our main results are summarized as follows:

(1) Throughput is generally increased by multi-hop transmissions, that is, low transmission power, except for sparse networks under moderate traffic loads. As the network density decreases, the multi-hop path covers a longer distance because

Table III. Routing strategy which maximizes goodput and throughput performances under different network and traffic conditions.

Goodput		Traffic load		
		Low	Moderate	High
Network size	Small-to-medium (N≤100)	single-hop	single-hop	single-hop
	Large (N>100)	single-hop or multi-hop	multi-hop	single-hop

Throughput		Traffic load		
		Low	Moderate	High
Network size	Small (N≤10)	multi-hop	single-hop	multi-hop
	Medium-to-large (N>10)	multi-hop	multi-hop	multi-hop

of path inefficiency [7], introducing more interference than single-hop routing. Consequently, the link layer throughput of multi-hop transmission becomes lower at moderate traffic loads where interference increases because of parallel transmissions.

(2) Goodput is increased by single-hop routing in sparse networks. This is due to path inefficiency of multi-hop routes where there are small number of alternative multi-hop routes and some of the links along the routes may be longer.

(3) Single-hop routing achieves higher goodput under heavy traffic loads, where goodput performance drops sharply with multi-hop transmissions, whereas throughput performance saturates. The reason behind these different behaviors is that goodput is the end-to-end data transfer rate, where only successfully received packets at the final destinations are counted. Although successful link transmissions occur under heavy traffic, end-to-end goodput substantially suffers from congestion losses because of increased traffic with multi-hop routing.

The routing strategy that maximizes the goodput and throughput performances under various regimes are summarized in Table III. The goodput and throughput performances of the studied IEEE 802.11 multi-hop networks show that adaptive selection of single-hop or multi-hop routing strategy based on the topology and the current traffic load may increase goodput considerably in multi-hop wireless networks.

As a future work, the analytical model can be improved by removing the assumption of using a common collision probability for the network, which reduces the accuracy of the results especially for small networks. This can be accomplished by generalizing the collision probability from a scalar to a vector.

REFERENCES

1. Gupta P, Kumar PR. The capacity of wireless networks. *IEEE Transactions on Information Theory* 2000; **46**(2): 388–404.
2. Xu S, Saadawi T. Does the IEEE 802.11 MAC protocol work well in multihop wireless adhoc networks? *IEEE Communications Magazine* 2001; **39**(6): 130–137.
3. Xu B, Hischke S, Walke B. The role of ad hoc networking in future wireless communications. In *International Conference on Communication Technology Proceedings (ICCT 2003)*, Beijing, China, 2003; 1353–1358.
4. Frey M, Grose F, Gunes M. Energy-aware ant routing in wireless multi-hop networks. In *IEEE International Conference on Communications (ICC)*, Sydney, Australia, 2014; 190–196.
5. Hahm O, Gunes M, Juraschek F, Blywis B, Schmittberger N. An experimental facility for wireless multi-hop networks in future internet scenarios. In *IEEE International Conference on Internet of Things (iThings/CPSCom)*, Dalian, China, 2011; 48–57.
6. Glaropoulos I, Mangold S, Vukadinovic V. Enhanced IEEE 802.11 power saving for multi-hop toy-to-toy communication. In *IEEE International Conference on Internet of Things (iThings/CPSCom)*, Beijing, China, 2013; 603–610.
7. Haenggi M, Puccinelli D. Routing in ad hoc networks: A case for long hops. *IEEE Communications Magazine* 2005; **43**(10): 93–101.
8. Ci S, Sharif H. Improving goodput in IEEE 802.11 wireless LANs by using variable size and variable rate (VSVR) schemes. *Wireless Communications and Mobile Computing* 2005; **5**(3): 329–342.
9. Aydogdu C, Karasan E. An analysis of IEEE 802.11 DCF and its application to energy-efficient relaying in multihop wireless networks. *IEEE Transactions on Mobile Computing* 2011; **10**(10): 1361–1373.
10. Goldsmith AJ, Wicker SB. Design challenges for energy-constrained ad hoc wireless networks. *IEEE Wireless Communications Magazine* 2002; **9**(4): 8–27.
11. Toumpis S, Goldsmith A. Capacity regions for ad hoc networks. *IEEE Transactions on Wireless Communications* 2003; **2**(4): 736–48.
12. Behzad A, Rubin I. High transmission power increases the capacity of ad hoc wireless networks. *IEEE Transactions on Wireless Communication* 2006; **5**(1): 156–165.
13. Park SJ, Sivakumar R. Quantitative analysis of transmission power control in wireless ad-hoc networks. In *Proceedings of International Conference on Parallel Processing Workshops*, Vancouver, British Columbia, Canada, 2002; 56–63.
14. Wang Y, Lui JCS, Chiu DM. Understanding the paradoxical effects of power control on the capacity of

wireless networks. *IEEE Transactions on Wireless Communications* 2009; **8**(1): 406–413.
15. Ramaiyan V, Kumar A, Altman E. Optimal hop distance and power control for a single cell, dense, ad hoc wireless network. *IEEE Transactions on Mobile Computing* 2012; **11**(11): 1601–1612.
16. Andrews JG, Weber S, Kountouris M, Haenggi M. Random access transport capacity. *IEEE Transactions on Wireless Communications* 2010; **9**(6): 2101–2111.
17. Nardelli PHJ, Cardieri P, Latva-aho M. Efficiency of wireless networks under different hopping strategies. *IEEE Transactions on Wireless Communications* 2012; **11**(1): 15–20.
18. Yang JW, Kwon JK, Hwang HY, Sung DK. Goodput analysis of a WLAN with hidden nodes under a non-saturated condition. *IEEE Transactions on Wireless Communications* 2009; **8**(5): 2259–2264.
19. Qui L, Zhang Y, Wang F, Han MK, Mahajan R. A general model of wireless interference. In *Proceedings of the ACM/IEEE International Conference on Mobile Computing and Networking (Mobicom)*, Montreal, Canada, 2007; 171–182.
20. Jang B, Sichitiu ML. IEEE saturation throughput analysis in presence of hidden terminals. *IEEE/ACM Transactions on Networking* 2012; **20**(2): 557–570.
21. Du W, Li M, Lei J. CO-MAP: improving mobile multiple access efficiency with location input. *IEEE Transactions on Wireless Communications* 2014; **PP** (99): 1–13.
22. Alizadeh-Shabdiz F, Subramaniam S. Analytical models for single-hop and multi-hop ad hoc networks. *Mobile Networks and Applications* 2006; **11** (1): 75–90.
23. Barowski Y, Biaz S, Agrawal P. Towards the performance analysis of IEEE 802.11 in multi-hop ad-hoc networks. In *IEEE Wireless Communications and Networking Conference*, New Orleans, USA, 2005; 100–106.
24. Tsertou A, Laurenson DI. Revisiting the hidden terminal problem in a CSMA/CA wireless network. *IEEE Transactions on Mobile Computing* 2008; **7**(7): 817–831.
25. Ng PC, Liew SC. Throughput analysis of IEEE 802.11 multi-hop ad hoc networks. *IEEE/ACM Transactions on Networking* 2007; **15**(2): 309–322.
26. Hira MM, Tobagi FA, Medepalli K. Throughput analysis of a path in an IEEE 802.11 multihop wireless network. In *IEEE Wireless Communications and Networking Conference (WCNC 2007)*, Hong Kong, China, 2007; 441–446.
27. Wang K, Yan F, Zhang Q, Xu Y. Modeling path capacity in multi-hop IEEE 802.11 networks for QoS services. *IEEE Transactions on Wireless Communications* 2007; **6**(2): 738–749.
28. Yang Y, Hou JC, Kung LC. Modeling the effect of transmit power and physical carrier sense in multi-hop wireless networks. In *Proceedings of* 26^{th} *IEEE International Conference on Computer Communications (infocom 2007)*, Alaska, USA, 2007; 2331–2335.
29. Giustiniano D, Malone D, Leith DJ, Papagiannaki K. Measuring transmission opportunities in 802.11 links. *IEEE/ACM Transactions on Networking* 2010; **18**(5): 1516–1529.
30. Bianchi G. Performance analysis of IEEE 802.11 distributed coordination function. *IEEE Journal on Selected Areas in Communications* 2000; **18**(3): 535–547.
31. Hwang IS, Chen CA. Saturation throughput analysis in IEEE 802.11 DCF using semi-markov model. *International Mathematical Journal* 2006; **1**(6): 289–296.
32. Duffy K, Malone D, Leith DJ. Modeling the 802.11 distributed coordination function in non-saturated heterogeneous conditions. *IEEE/ACM Transactions on Networking* 2007; **15**(1): 159–172.
33. Ray S, Starobinski D. On false blocking in RTS/CTS-based multi-hop wireless networks. *IEEE Transactions on Vehicular Technology* 2007; **56**(2): 849–862.
34. Wireless LAN medium access control (MAC) and physical layer (PHY) specifications. *Technical Report Std 802.11, R2003*, ANSI/IEEE, 1999.
35. Gross D, Harris CM. *Fundamentals of queueing theory* (2^{nd}), Wiley Series in Probability and Mathematical Statistics. John Wiley & Sons Ltd.: New York, 1985.
36. The network simulator ns-2. [Online]. Available: http://nsnam.isi.edu/nsnam/index.php/Main_Page [Accessed on 27 April 2015].
37. Adame T, Bel A, Bellalta B, Barcelo J, Oliver M. IEEE 802.11ah: the WiFi approach for M2M communications. *IEEE Wireless Communications* 2014; **21**(6): 144–152.

AUTHORS' BIOGRAPHIES

Canan Aydogdu received her BS degrees with honors both in Electrical and Electronics Engineering Department and Physics Department in 2001 from Boğaziçi University, Istanbul, Turkey, and MS degree in 2003 and Ph. D. degree in 2010 in Electrical and Electronics Engineering from Bilkent University, Ankara, Turkey. She is currently with the Department of Electrical and Electronics Engineering at İzmir Institute of Technology. Her current work focuses on Bluetooth, IEEE 802.11 and energy-conserving protocols in wireless ad hoc and sensor networks.

Ezhan Karasan received B.S. degree from Middle East Technical University, Ankara, Turkey; M.S. degree from Bilkent University, Ankara, Turkey; and Ph.D. degree from Rutgers University, Piscataway, New Jersey, USA, all in electrical engineering, in 1987, 1990, and 1995, respectively. During 1995–1996, he was a post-doctorate researcher at Bell Labs, Holmdel, New Jersey, USA. From 1996 to 1998, he was a senior technical staff member at AT&T Labs-Research, Red Bank, New Jersey. He has been with the Department of Electrical and Electronics Engineering at Bilkent University since 1998. Dr. Karasan is a member of the Editorial Board of Optical Switching and Networking journal. He is the recipient of 2004 Young Scientist Award from Turkish Scientific and Technical Research Council (TUBITAK), 2005 Young Scientist Award from Mustafa Parlar Foundation, and Career Grant from TUBITAK in 2004.

Wirel. Commun. Mob. Comput. 2016; **16**:1078–1094 © 2015 John Wiley & Sons, Ltd.
DOI: 10.1002/wcm